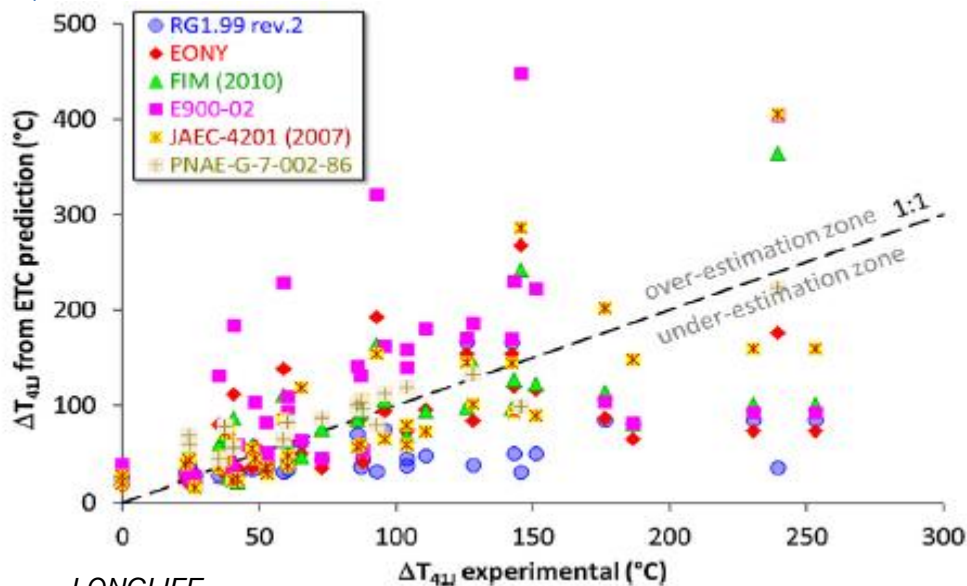


# EFFECT OF MATERIALS HETEROGENEITIES ON MECHANICAL PROPERTIES AT INITIAL STATE

Marta Serrano García



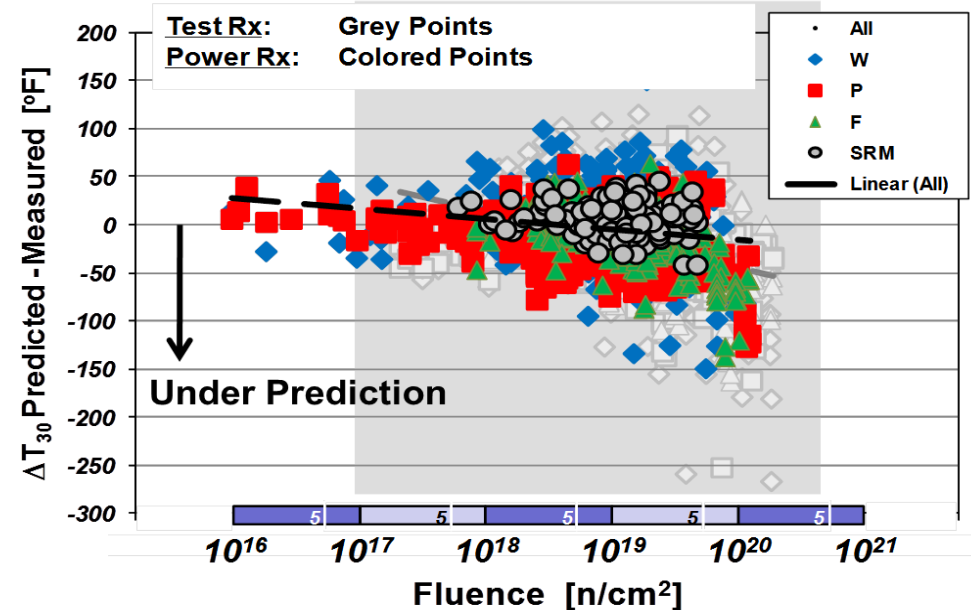
- Existing ETC do are not accurate to predict embrittlement at high fluences and/or low Cu materials



LONGLIFE

E. Altstadt et al. / NED 278 (2014) 753–757

## 10 CFR 50.61 a Predictions Mark Kirk USNRC



- ❑ The scatter of the measured shift could come from
  - A inaccurate prediction of the ETC
  - Uncertainty of irradiation effects
  - Uncertainty on initial properties
- ❑ Included on  $RT_{NDT}$  shift as margin

$$\text{Margin} = 2\sqrt{\sigma_I^2 + \sigma_{\Delta}^2}$$

$\sigma_I$  is the standard deviation for the initial  $RT_{NDT}$  ( $T_{41J}$ )

$\sigma_{\Delta}$  is the standard deviation of  $\Delta RT_{NDT}$ :

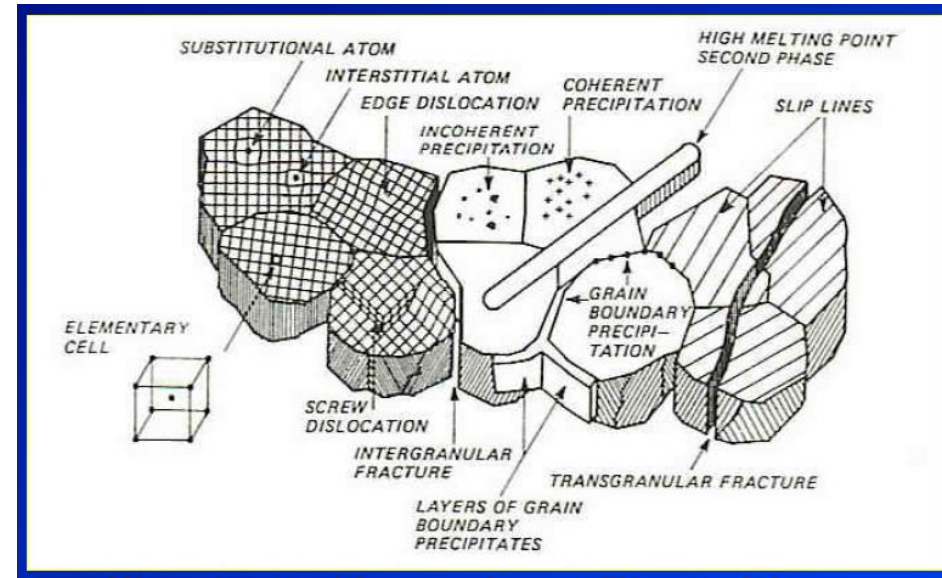
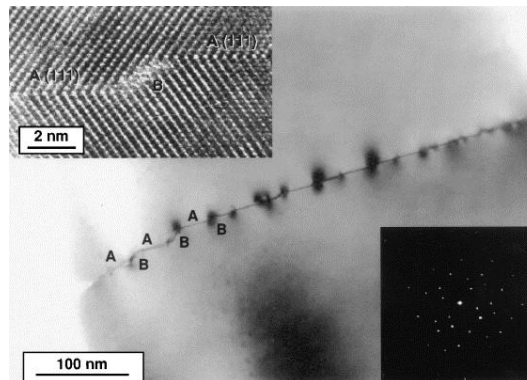
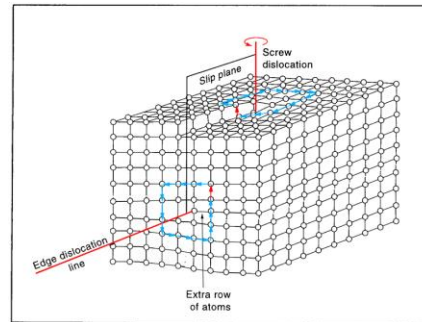
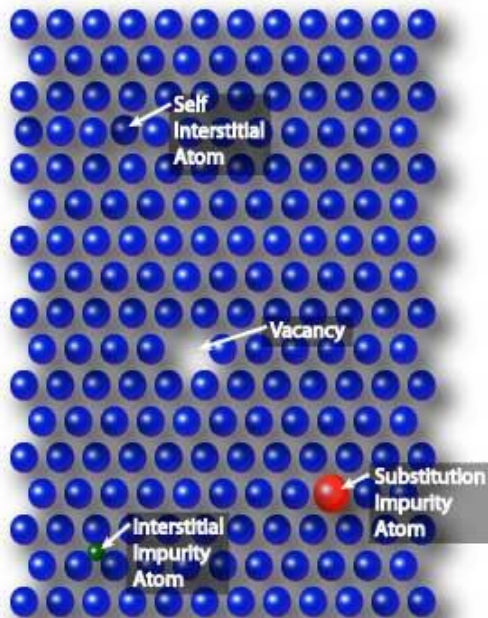
28°F for welds

17°F for base metal

Unnecessary conservatism can be reduced when the accuracy of the mean condition is increased and the contributions to the total margin are properly understood

This presentation is focused on the **initial state**

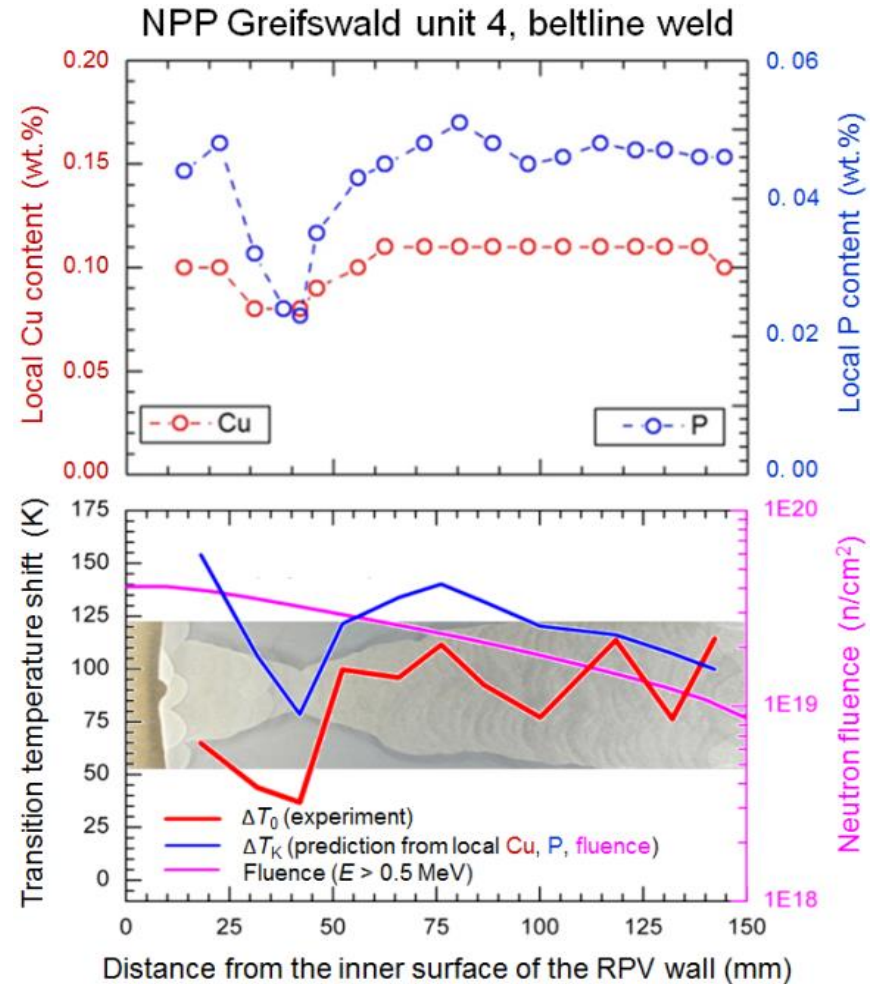
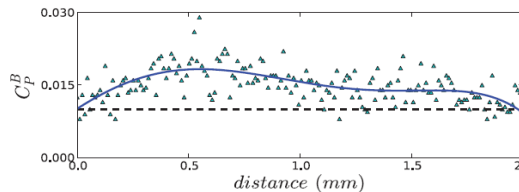
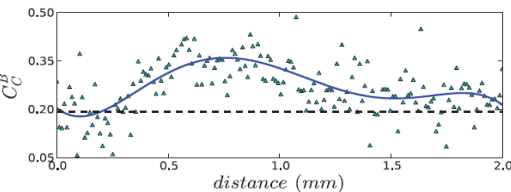
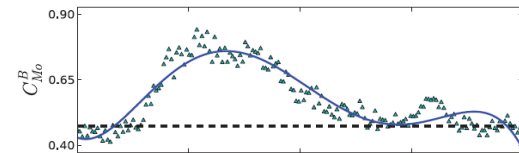
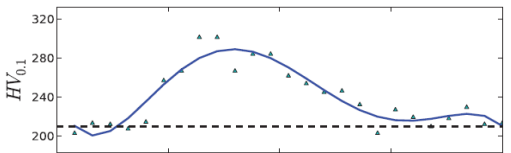
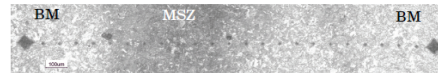
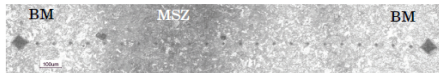
- ❑ Most engineering materials are inherently inhomogeneous in their processing, internal structure, properties, and performance.
- ❑ Their properties are therefore statistical rather than deterministic
- ❑ These inhomogeneities manifest across multiple length



□ Inhomogeneity usually comes from the fabrication procedure

- Casting - Forging
- Welding
- Surface finishing
- Final heat treatment

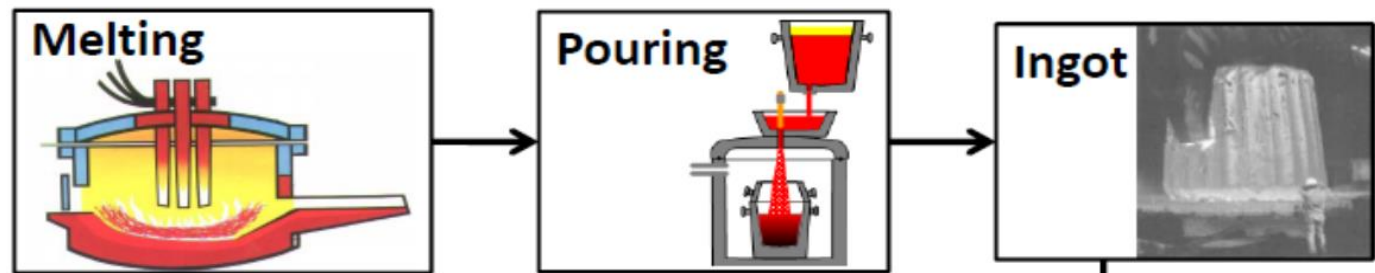
Antoine Andrieu et al. / *Procedia Materials Science* 3 (2014)



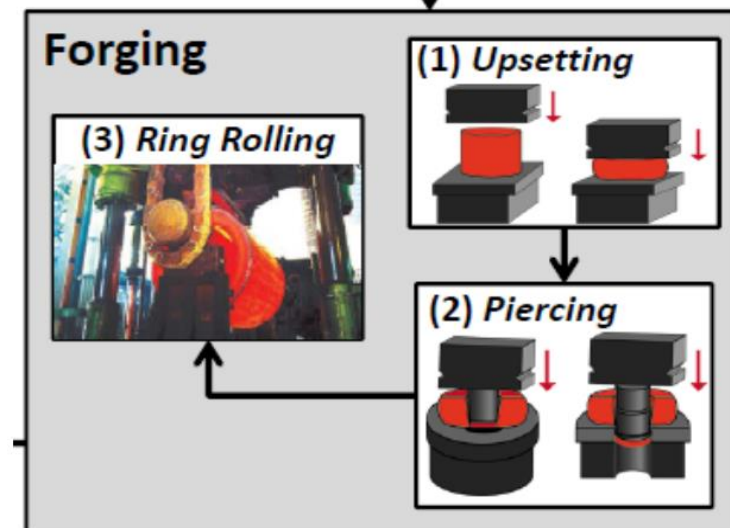
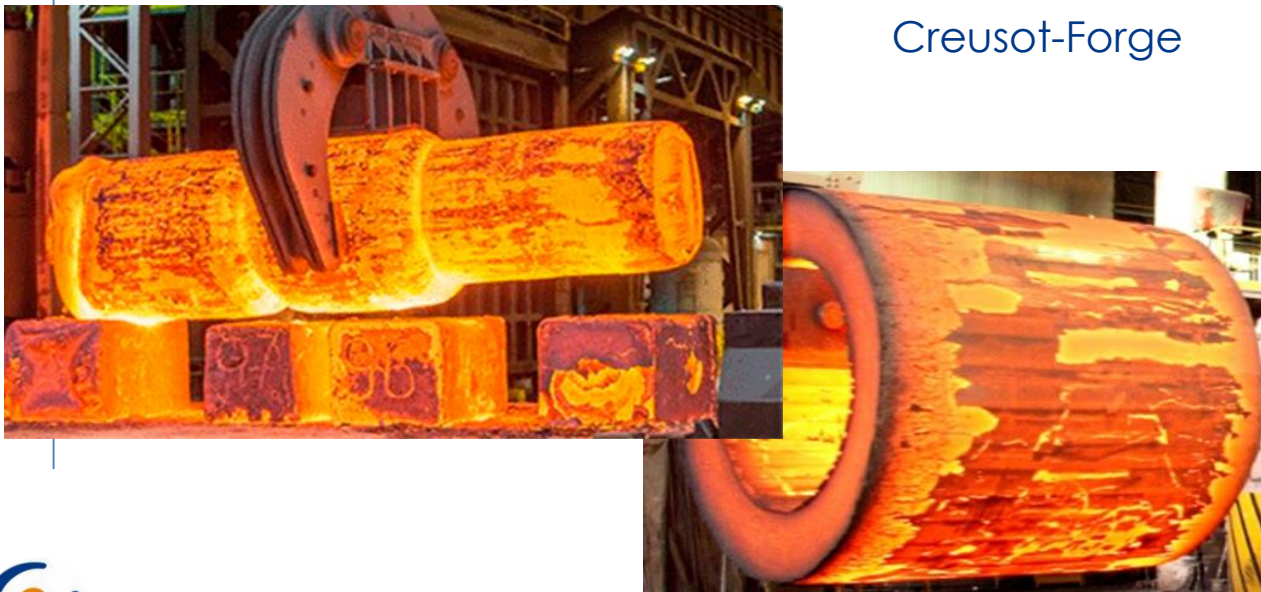
H.-W. Viehrig (HZDR) LONGLIFE

## ❑ Forgings

- One potential origin of scatter can be segregation during the fabrication of the ingot due to **segregations**



Creusot-Forge

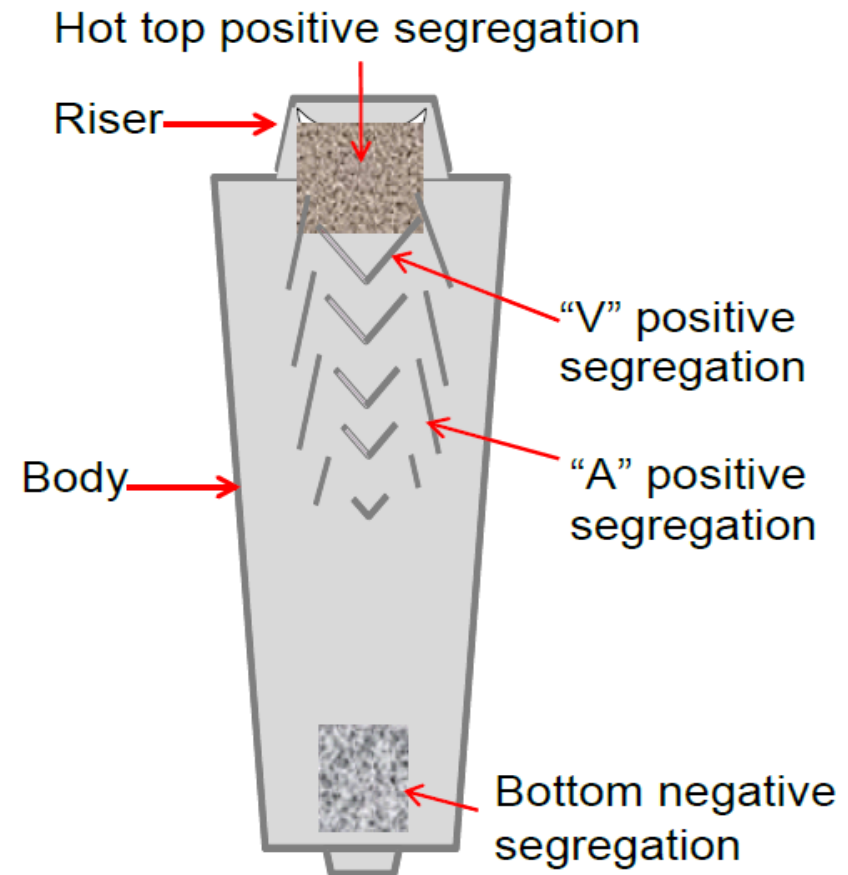


- ❑ Segregation refers to non-uniformity of chemical composition.
- ❑ Segregation can occur during solidification by multiple mechanisms and over different length scales
- ❑ **Microsegregation**
  - Occurs over distances on the order of the microstructure of the alloy.
  - The process of microsegregation is primarily controlled by diffusion in the liquid phase near the solidification front. The degree of microsegregation is dependent on the material composition and cooling rate.
  - It typically does not impact the performance of steel forgings because can be eliminated during the subsequent thermomechanical processing.
- ❑ **Macrosegregation**
  - Occurs in alloy castings or ingots ranges in scale from several millimeters to centimeters or even meters. ,
  - Cannot be removed by subsequent thermomechanical processing.
- ❑ Positive (negative) segregation refers to the composition above (below) the nominal composition

$$\frac{\Delta C}{C_0} = \frac{(C_i - C_0)}{C_0}$$

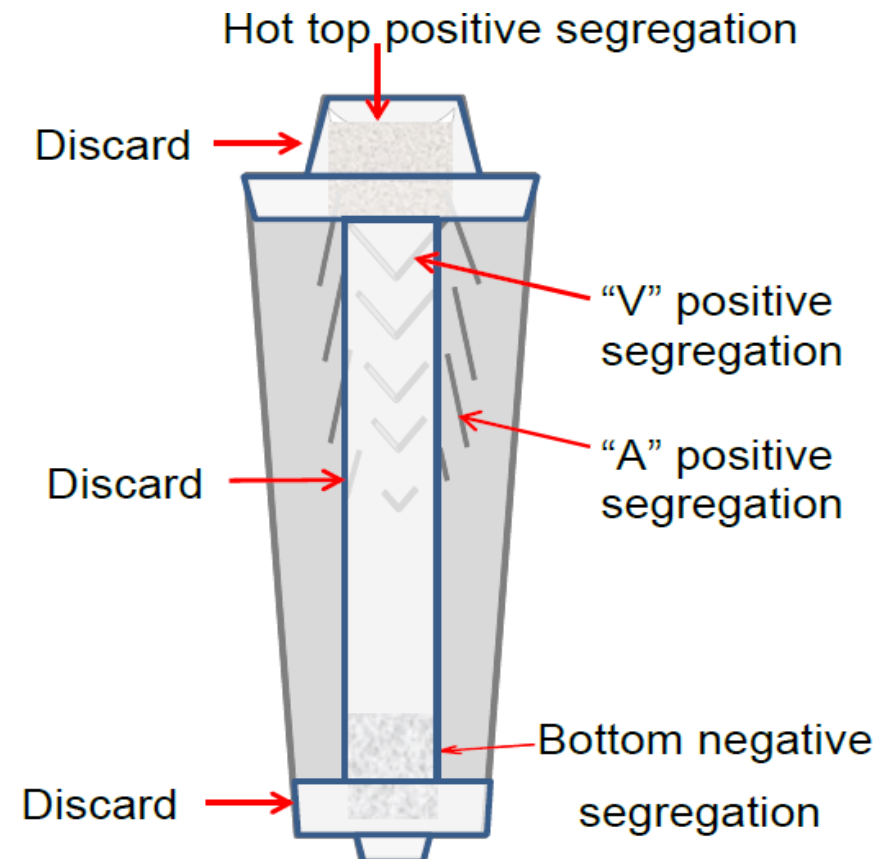
$C_0$  is the nominal composition of the material,  $C_i$  is the composition at a specific location in the material, and  $\Delta C$  is the local deviation from the nominal composition in weight percent(wt%) of the element

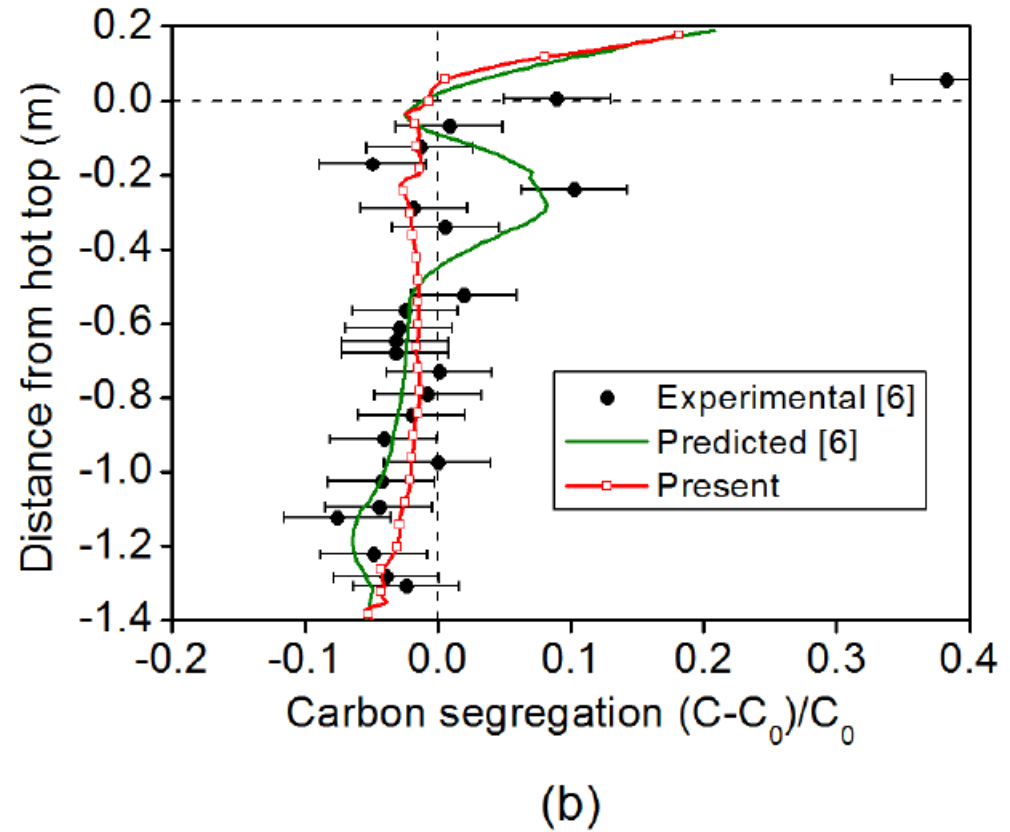
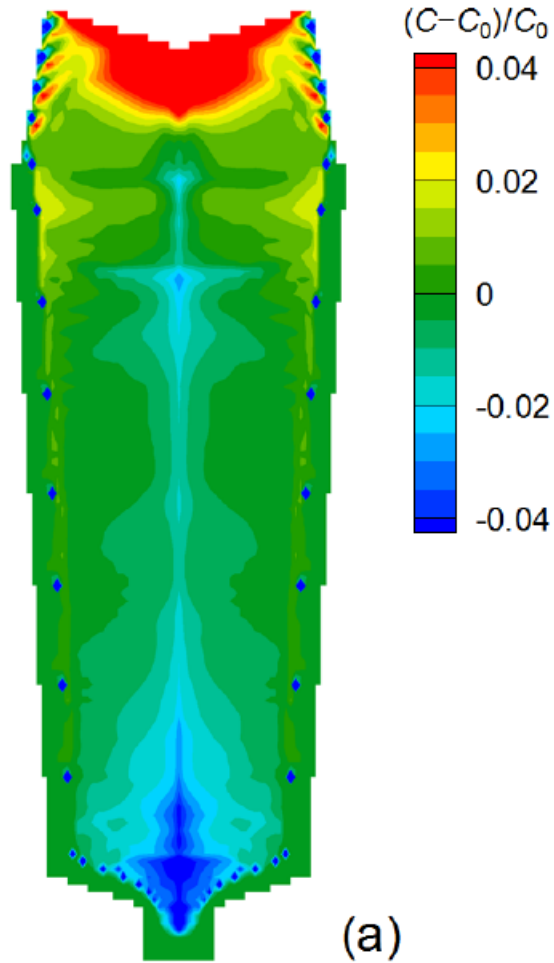
- ❑ At the end of the solidification the average element composition in the ingot is the same as the nominal value in the molten metal; however, the ingot now contains various defects and regions of heterogeneity, where the element contents either can be higher or lower than the nominal values.
- ❑ There are multiple types of macrosegregation that may occur during the casting of large steel ingots.
- ❑ The most relevant types include positive hot-top, negative cone, and positive channel (i.e., A-type, and V-type).



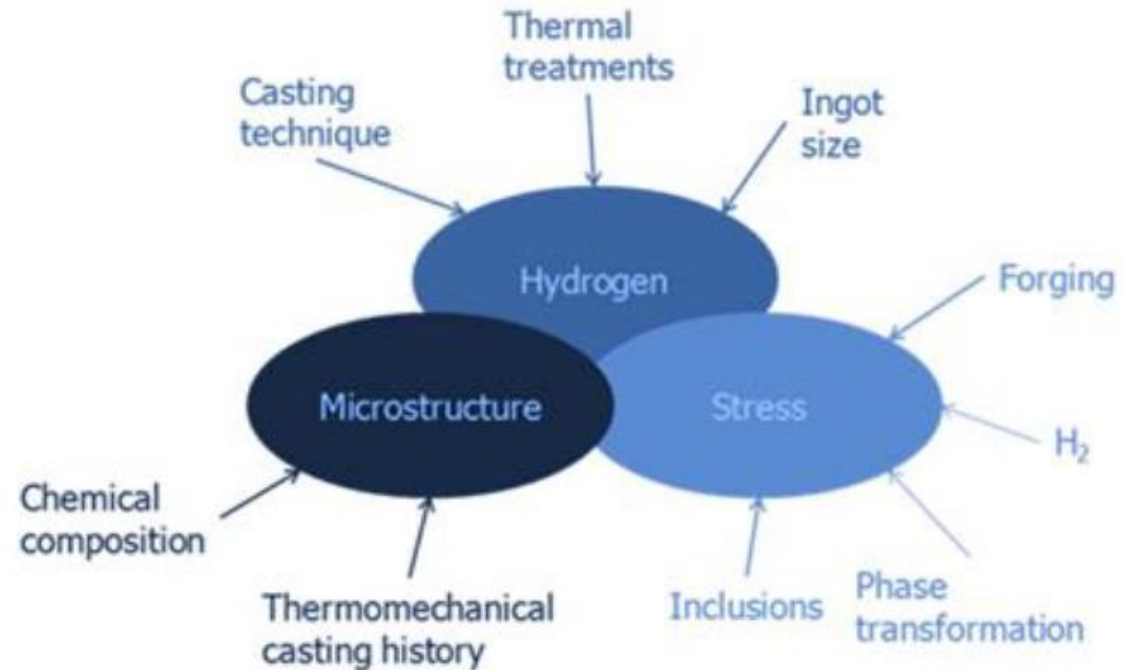


- ❑ If a ring is to be forged, then trepan forging is used to remove a core of material from the center of the forging; this process removes most of the “V” macrosegregation that is present in the center of the forging.
- ❑ Some of the “A” macrosegregation then will remain and extend along the length of the forging both at the surface and embedded in the wall. The portions of the ingot that are discarded and the carbon macrosegregation that is removed by the cropping and trepan forging operations
- ❑ If a head is to be forged, then the center is not trepanned, and the “A” and “V” segregates not removed by cropping the top of the ingot will remain in the forged component.





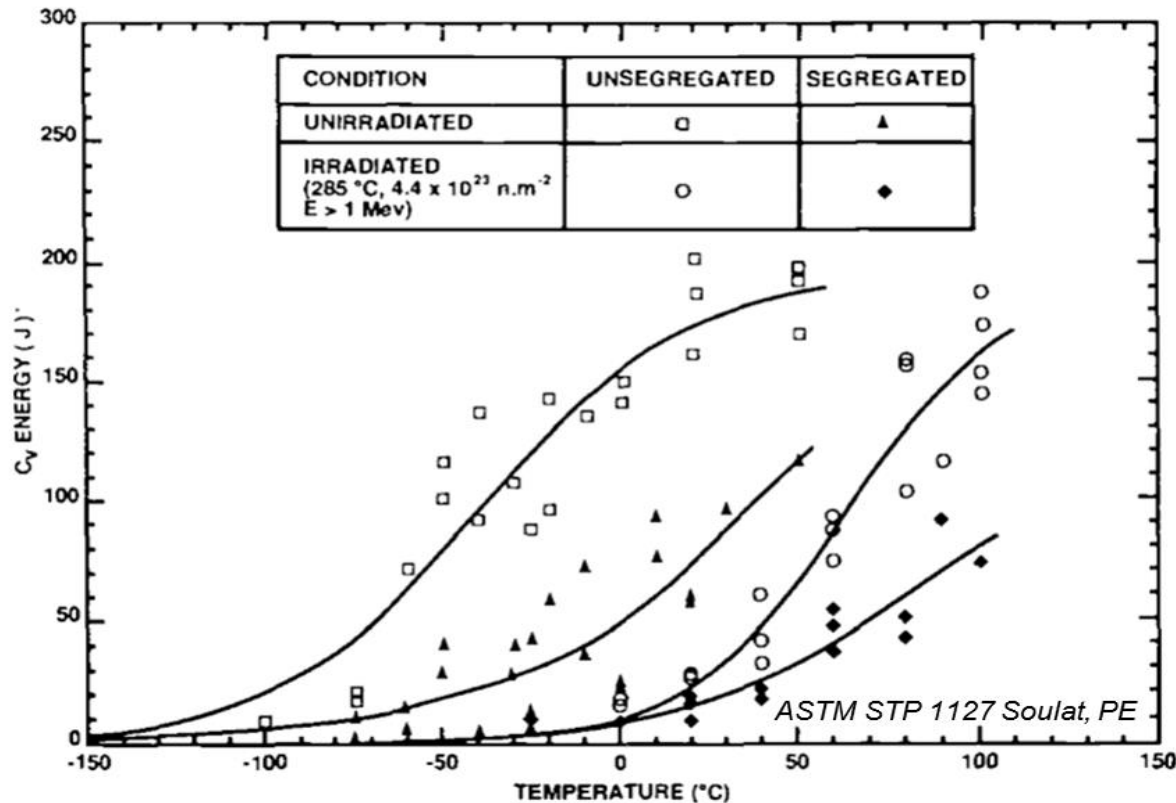
- ❑ The formation of hydrogen flakes is a phenomenon well known to the steel manufacturers and may happen after cooling down the steel from high to ambient temperature, in the ingot after pouring or in the forged part after the forging operation and heat treatment.
- ❑ Flake formation is driven by the accumulation of hydrogen at segregations or inclusions in the metal



<https://fanc.fgov.be>

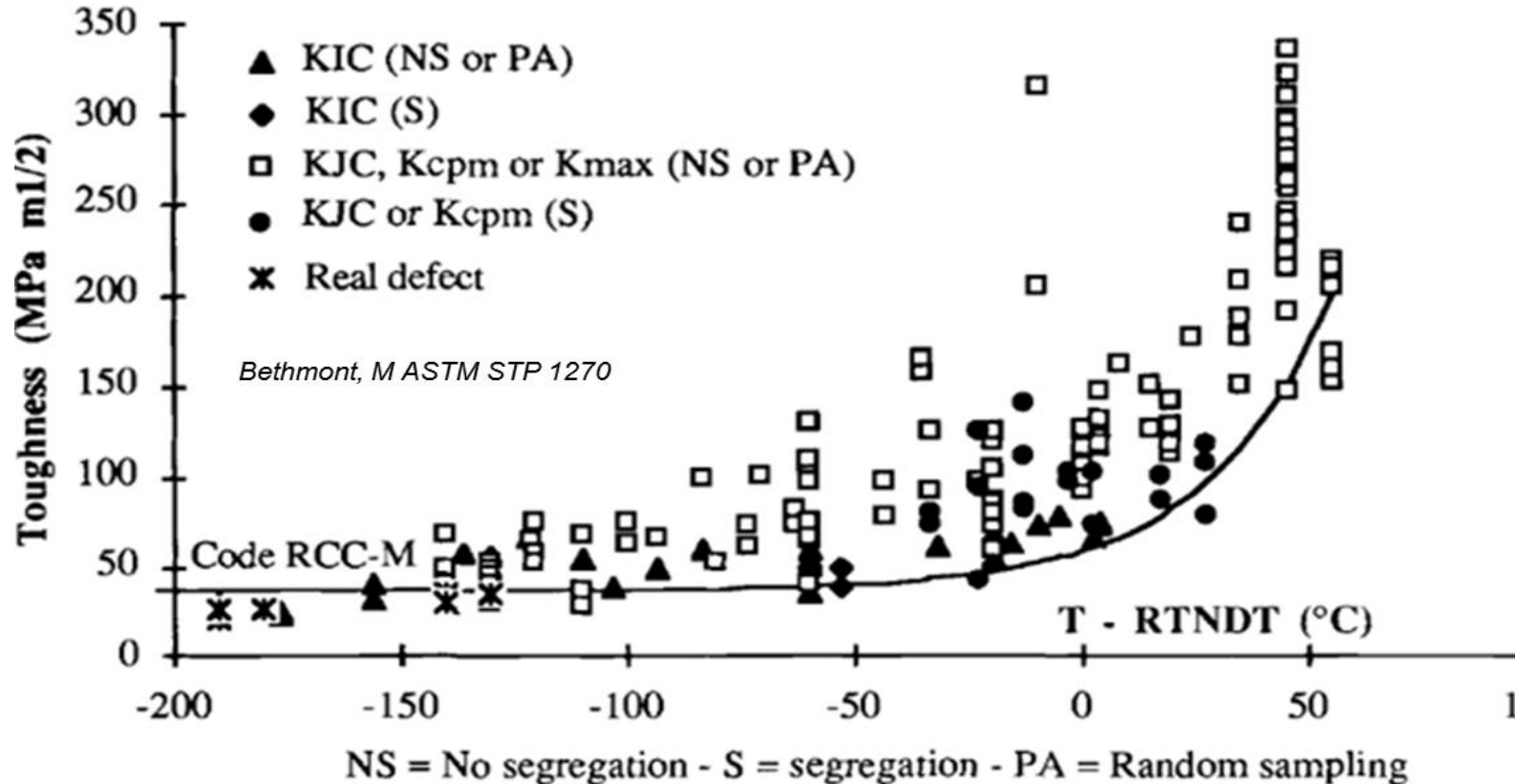
# Carbon segregation

- CVN energy (CV) plotted against test temperature for RPV material with and without regions of positive channel segregation
- The data exhibits a 75°C shift in the unirradiated  $RT_{NDT}$ , at the 68J energy level, for the segregated material.

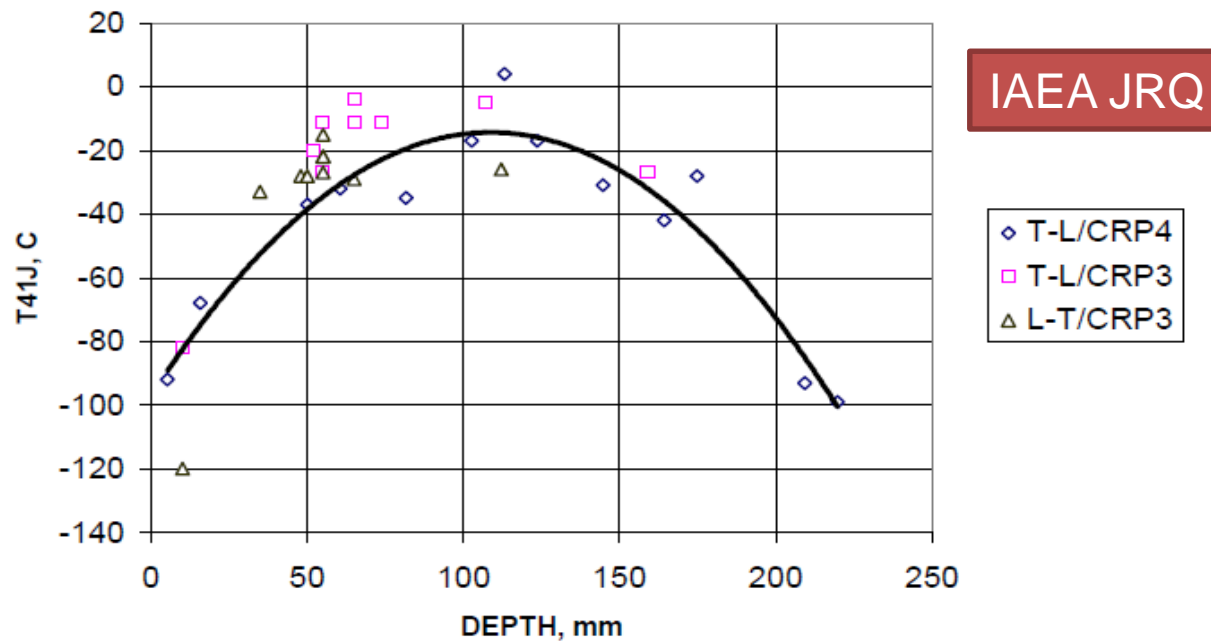


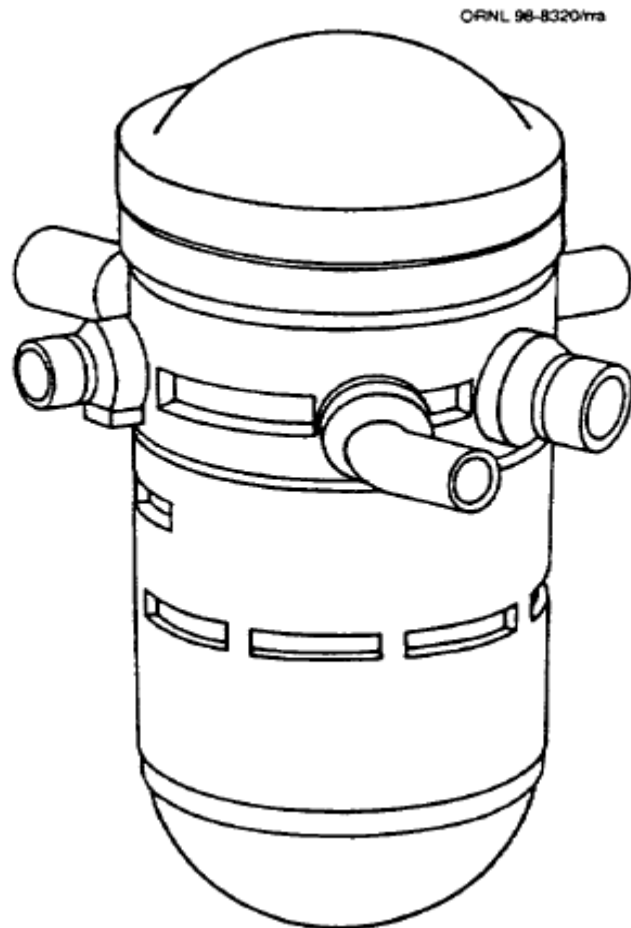
# Carbon segregation

- Fracture toughness plotted against the indexed temperature for RPV steel with and without regions of positive channel segregation

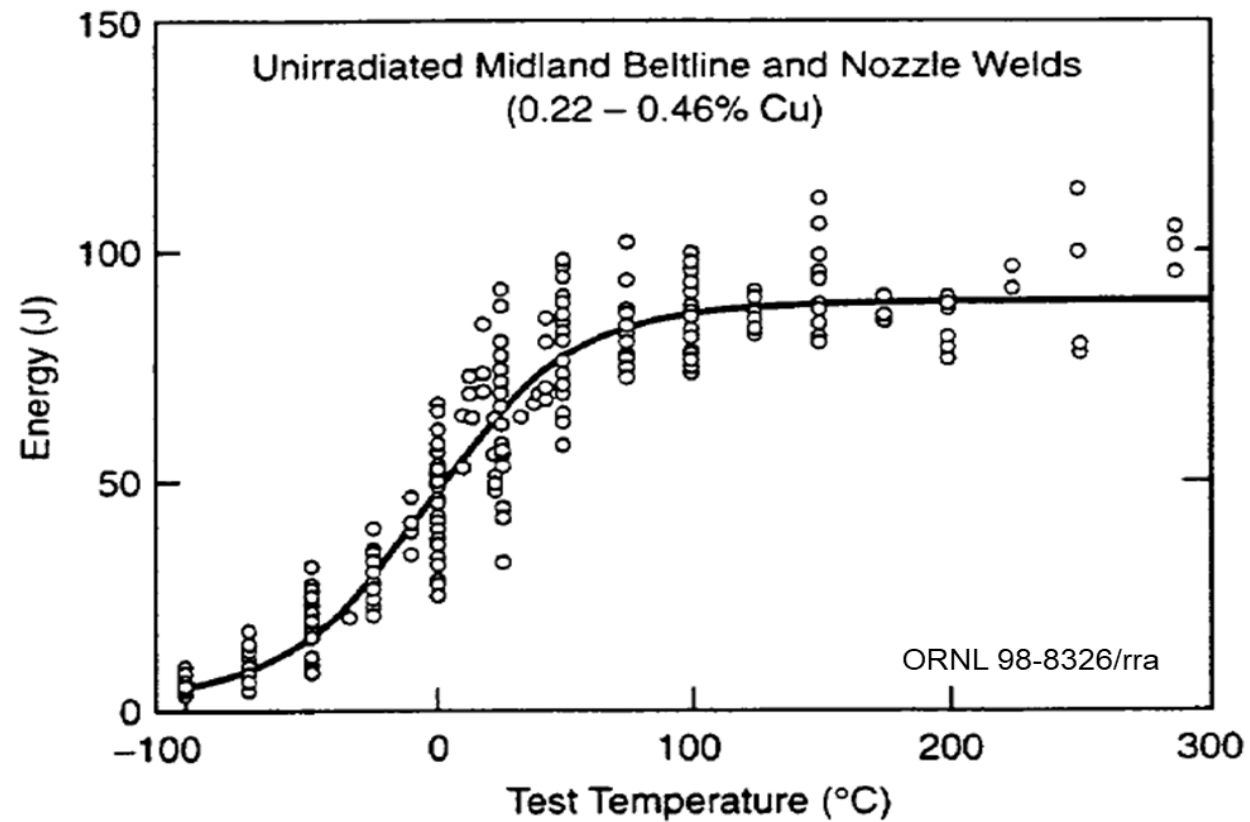


- ❑ Plate material is generally considered much less prone to carbon segregation due to smaller ingot sizes and higher degrees of deformation during the rolling operation compared to forging. This results in a less sensitive microstructure.
- ❑ Variation along thickness are mainly due to heat treatment



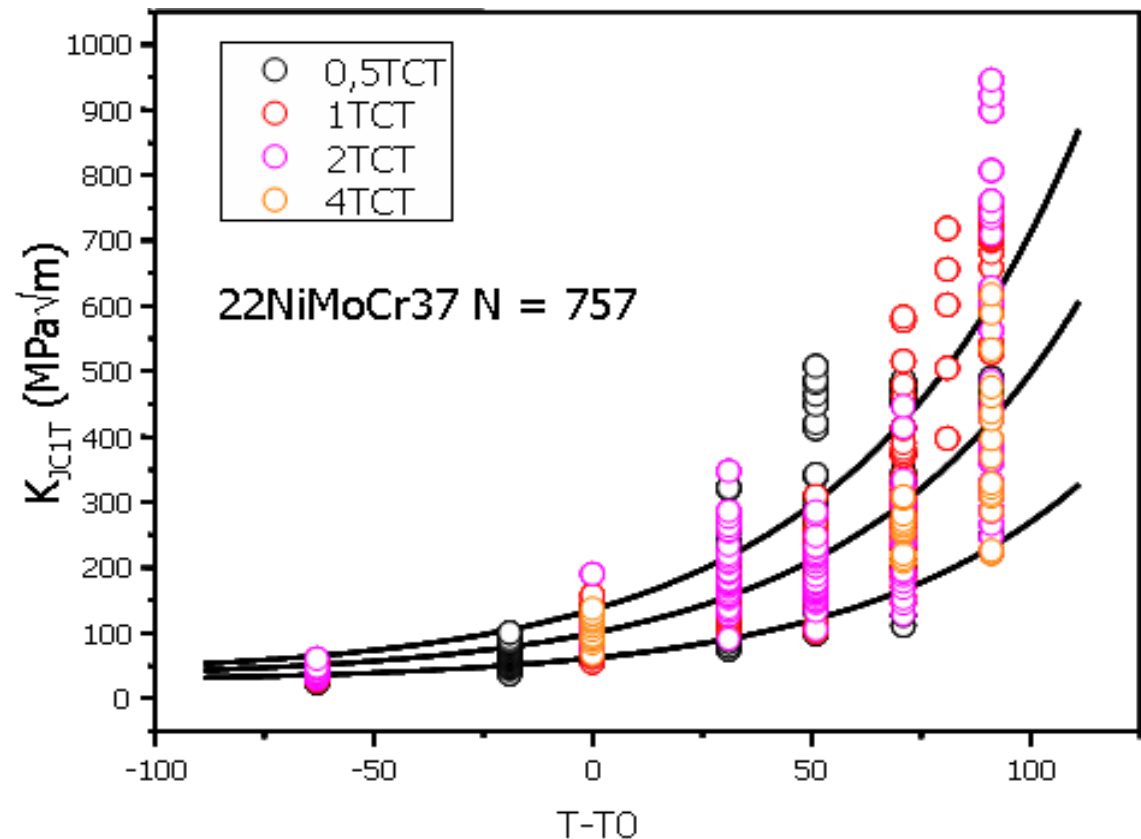
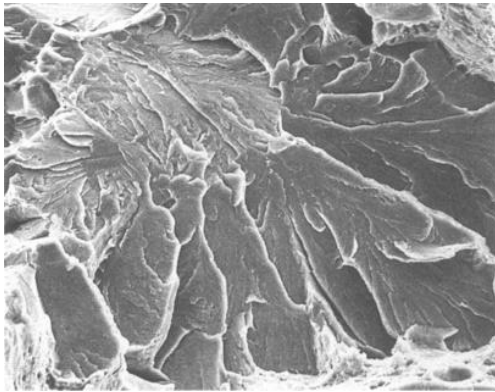


**Temperature of 41-J Charpy Energy Level Varied with Sampling Location  
(Similar Scatter Seen in HSSI Welds 72W and 73W)**



- The Master Curve describe the scatter in the transition region
- Cleavage Fracture

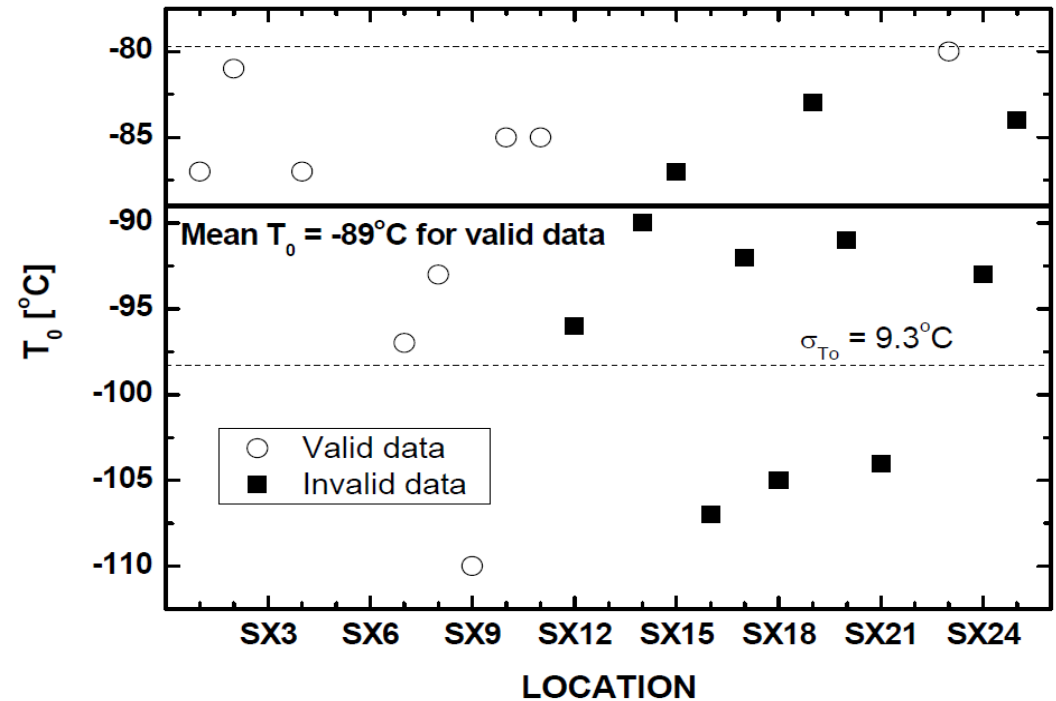
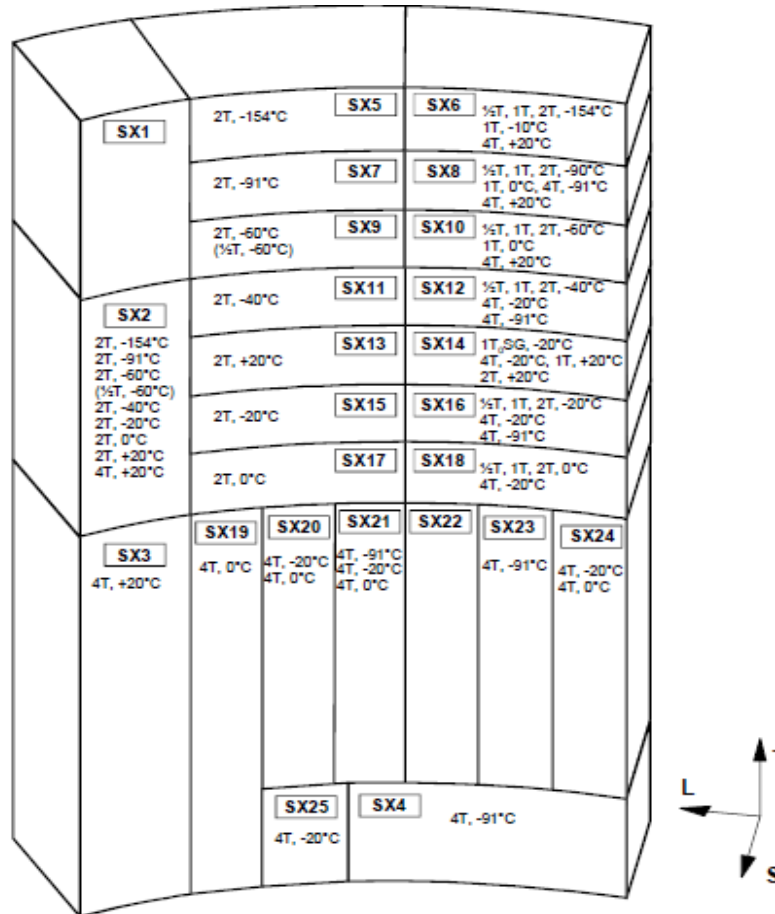
$$P_f = 1 - \exp\left(-\frac{B}{B_0} \left(\frac{K_{JC} - K_{min}}{K_0 - K_{min}}\right)^b\right)$$





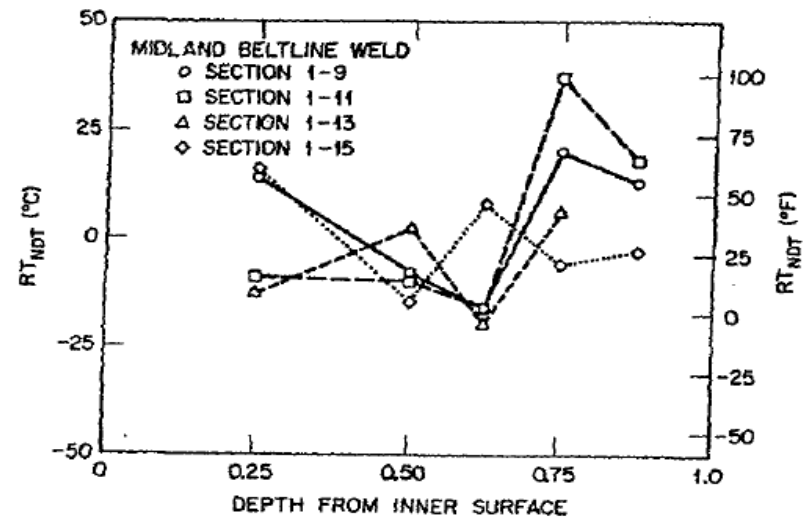
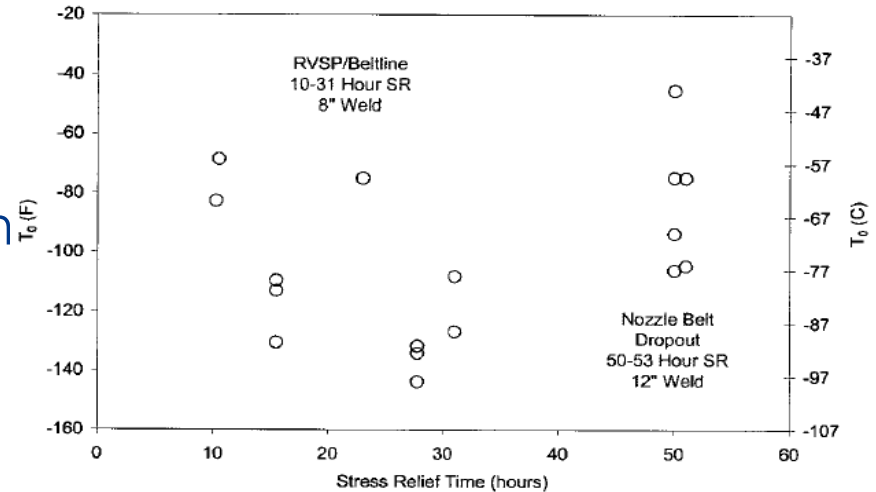
# Scatter in fracture toughness

## □ T<sub>0</sub> variations – Euro Master Curve



# Scatter in fracture toughness

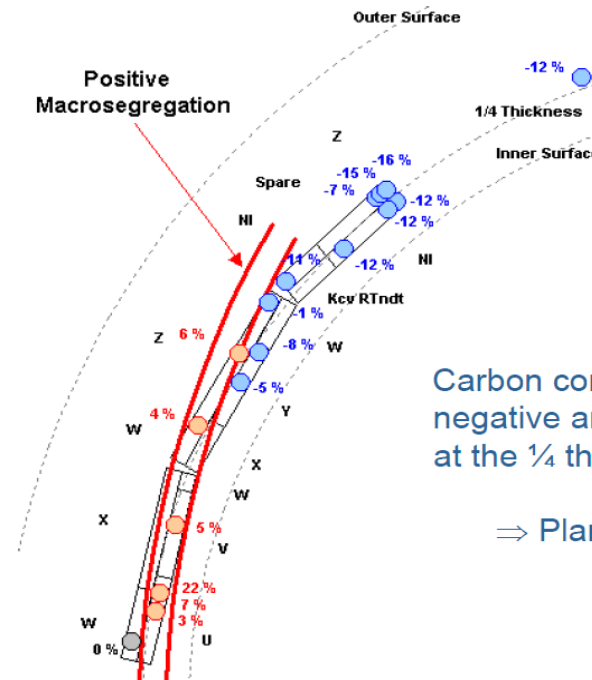
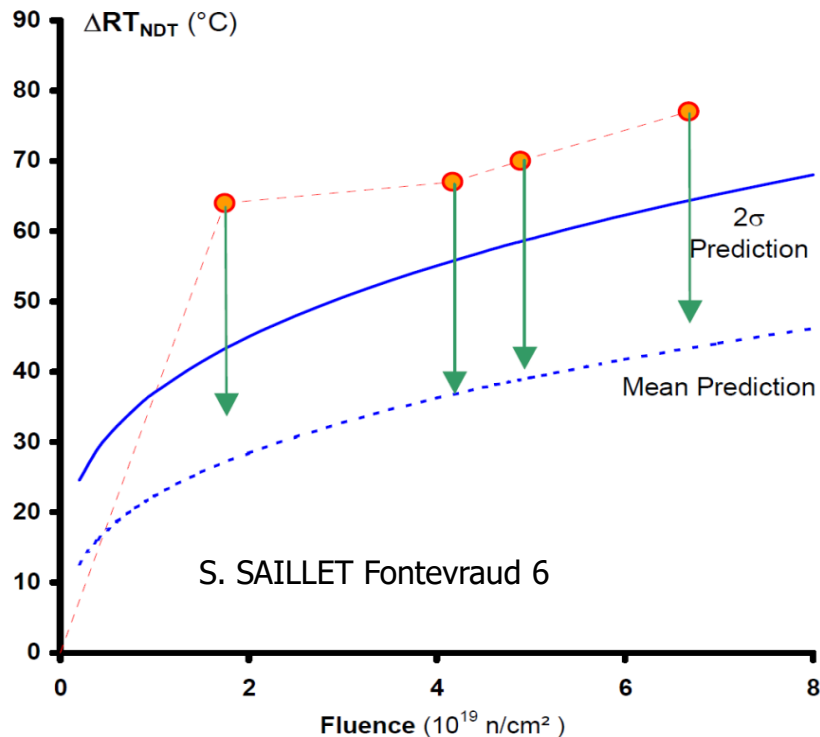
- ❑ The sources of variation on Master Curve reference temperature  $T_0$  can be grouped into two categories:
- ❑ Recognized sources of variation, which can be compensated for
  - 1) specimen loading rate,
  - 2) PCCS bias, and
  - 3) stress relief time/material source
- ❑ Other sources of variation compensated by the initial margin term
  - 1) testing laboratory,
  - 2) test procedure,
  - 3) material,
  - 4) sample size (number of specimens), and
  - 5) other.



# Examples

- ❑ EDF-AREVA large forgings project
- ❑ Surveillance results of a French NPP show atypical results – not related to irradiation
- ❑ Metallurgical heterogeneities

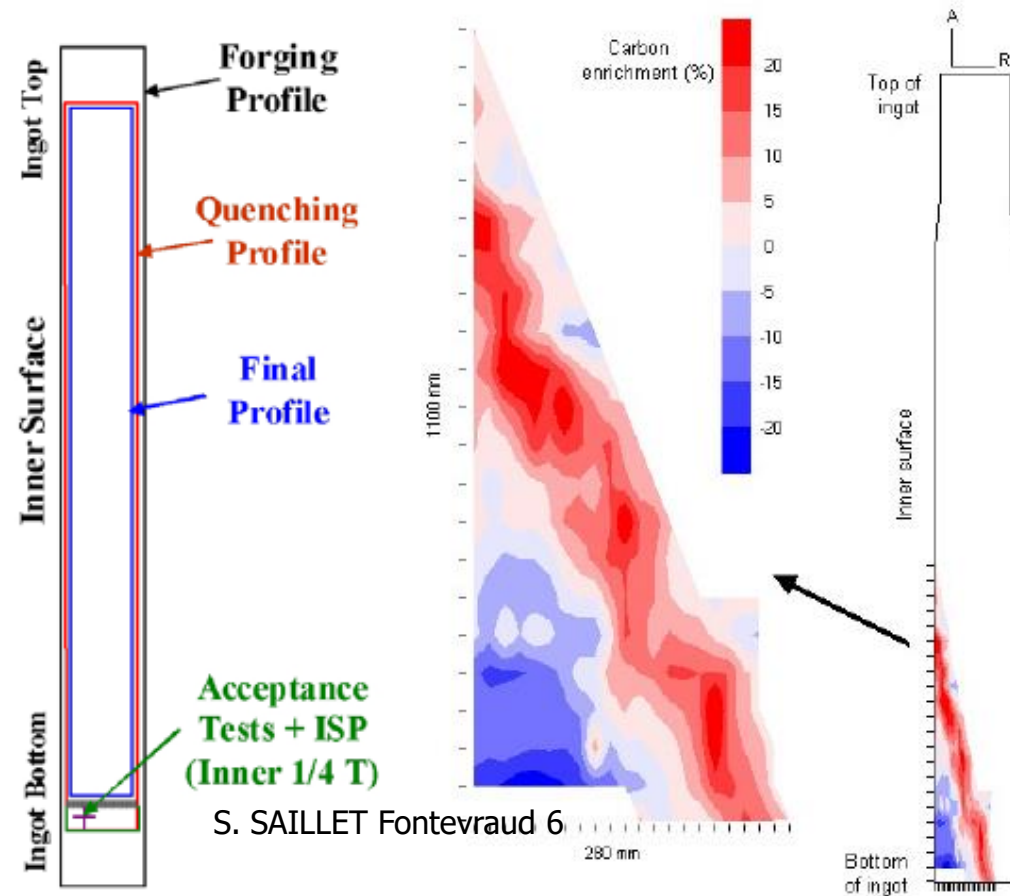
no excessive embrittlement of the material, but a bias between unirradiated and irradiated specimens populations



Carbon contents indicate the presence of negative and positive macrosegregations at the 1/4 thickness of the acceptance ring

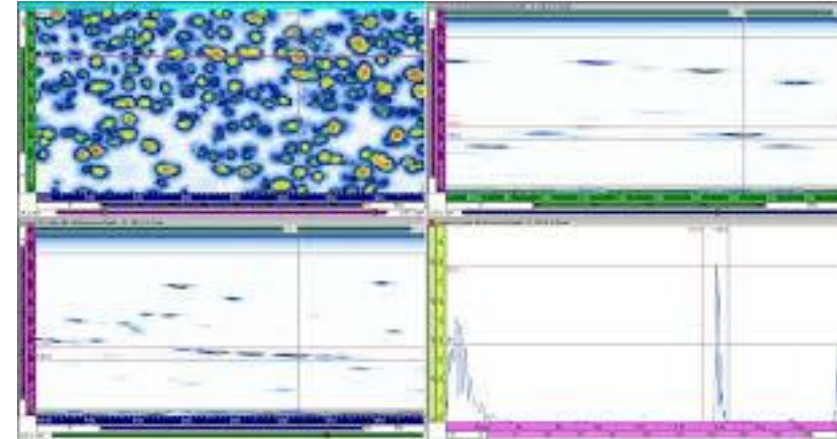
⇒ Plant A acceptance ring is not homogeneous

- ❑ Macro-segregation
- ❑ Acceptance test and irradiation surveillance program coupons are taken from the end corresponding to the bottom of the initial ingot
- ❑ Zones affected by positive segregation can locally be present at the internal skin of the core shells
- ❑ The quarter-thickness of the acceptance ring, where the PVSP specimens come from with zero or negative segregation.



## □ Doel and Tihange indications

- In June 2012 during regular maintenance shutdown of Doel 3 NPP an ultrasonic (UT) inspection was performed on the steel Reactor Pressure Vessel (RPV) -> a large number of “flaw indications” or micro cracks in the lower and upper reactor core shells were detected in the base metal
- Comparable, yet fewer, indications were found three months later in the Tihange 2 nuclear power plant after a similar inspection



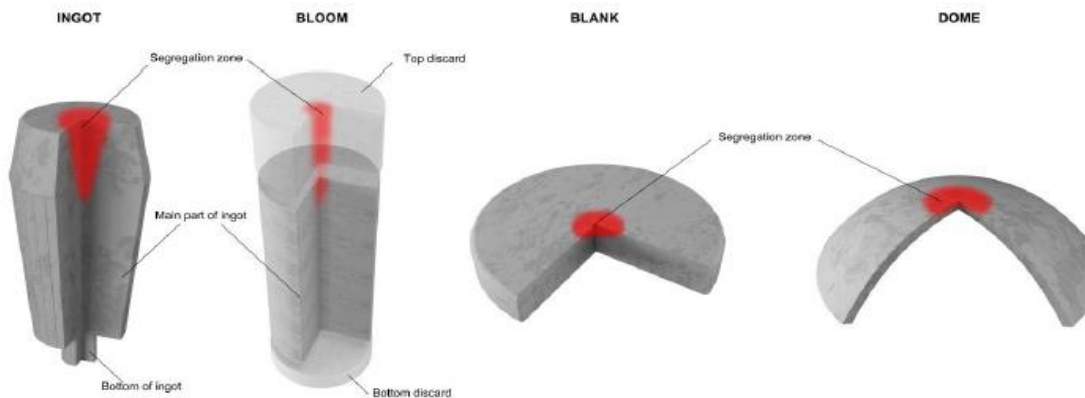
*D. Moussebois*

## Hydrogen flakes

- hydrogen flakes were initiated during manufacturing in macro-segregated areas, in particular in ghost lines at manganese sulphide inclusions.
- limited effect of hydrogen flaking on the material properties.

Structural integrity is demonstrated with significant safety margins

- ❑ The Flamanville EPR reactor pressure vessel closure head and bottom head domes were manufactured in 2006 and 2007 by forging
- ❑ At the end of 2014, Areva NP informed that the results of the impact tests were lower than expected
- ❑ The carbon concentration measurements taken at the surface of the upper dome revealed the presence of a residual positive macrosegregation zone over a diameter of about one meter.
- ❑ Furthermore, the examinations performed on the material sampled at depth, in the center of this dome, show that the segregation extends to a depth exceeding the half-thickness of the dome



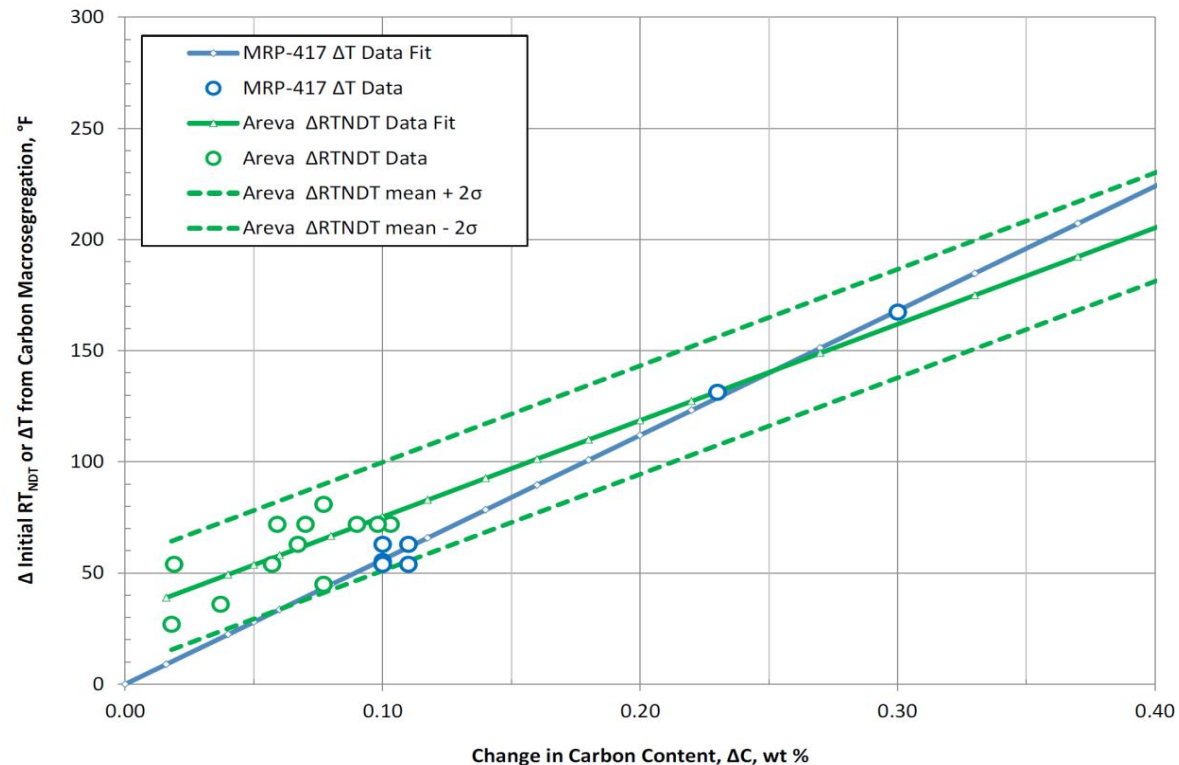
- ❑ The analyses carried out by EDF since 2015 conclude that certain steam generator channel heads could contain a zone comprising a high carbon concentration which could lead to lower than expected mechanical properties.
- ❑ A detailed analysis were carried out
- ❑ There are substantial margins against failure through an 80-year operating period when conservative distributions of carbon macrosegregation are postulated to be present in the RPV, S/G and pressurizer head and ring forgings in PWRs.



# Carbon macrosegregation

- EPRI assumed the  $RT_{NDT}$  changes per the following expression (MRP-471)
- $RT_{NDT(U)} = RT_{NDT(U_0)} + \Delta RT_{NDT(U)}$ 
  - $RT_{NDT(U_0)}$  is the unirradiated reference temperature for the material with carbon content equal to the nominal value in the ingot, Co.
  - $\Delta RT_{NDT(U)}$  is the change in  $RT_{NDT(U)}$  as a function the change in carbon content, °F (°C)/wt. % C, and is determined from experimental data.

$$\Delta RT_{NDT(U)} (\text{°C}) = 241.01 (\text{°C/wt. \% C}) \cdot \Delta C (\text{wt. \%}) + 17.83 (\text{°C}).$$



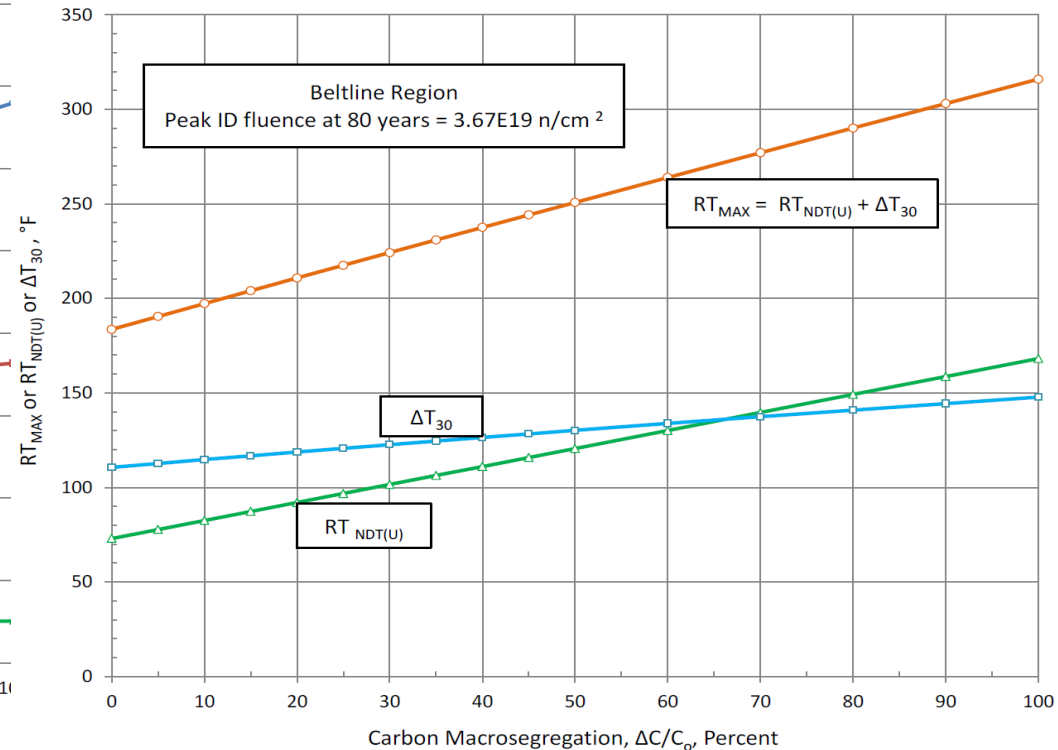
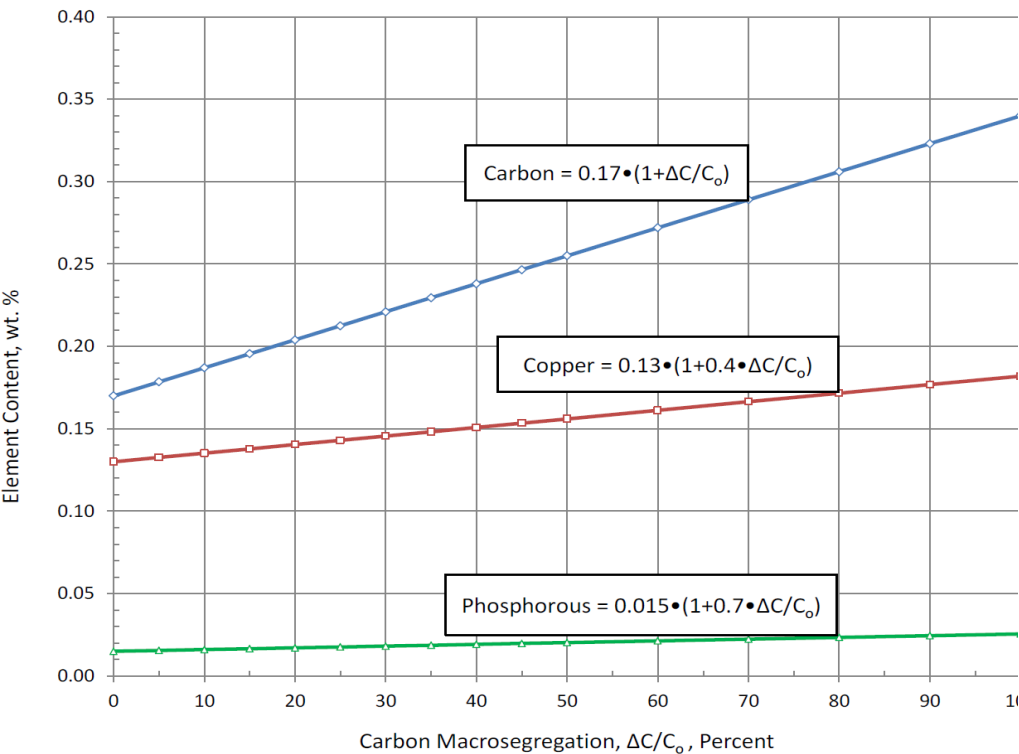
EPRI MRP-417



# Carbon macrosegregation



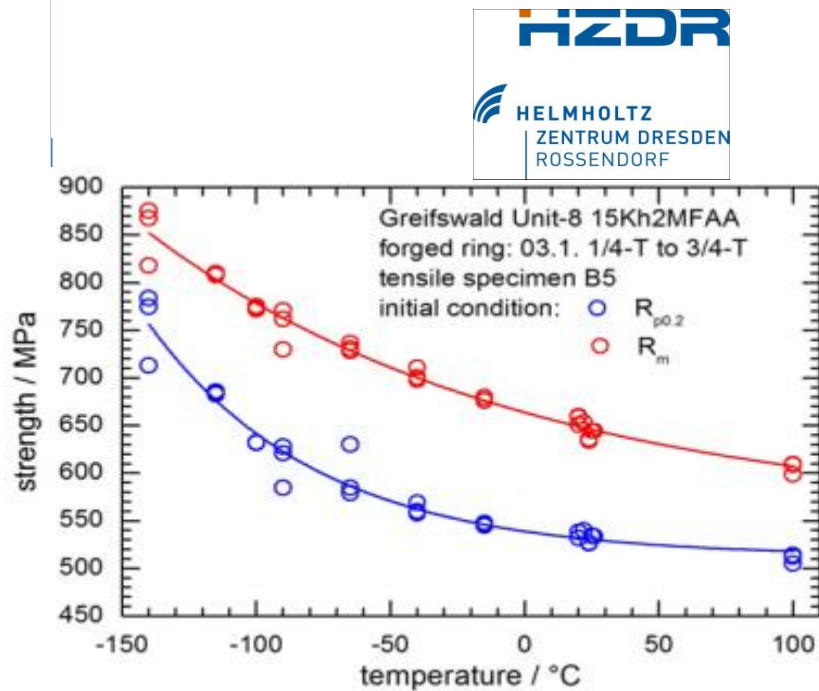
- When carbon macrosegregation occurs in large forgings it is accompanied by copper and phosphorus macrosegregation with increased **copper** and phosphorous



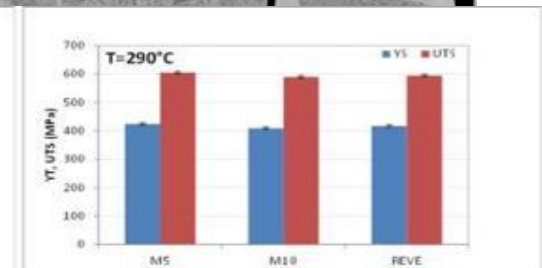
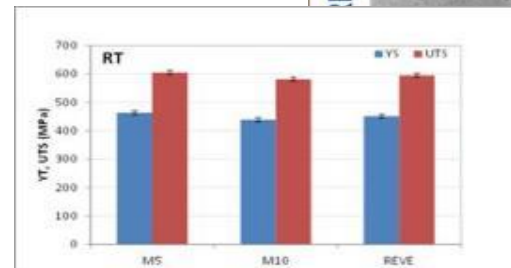
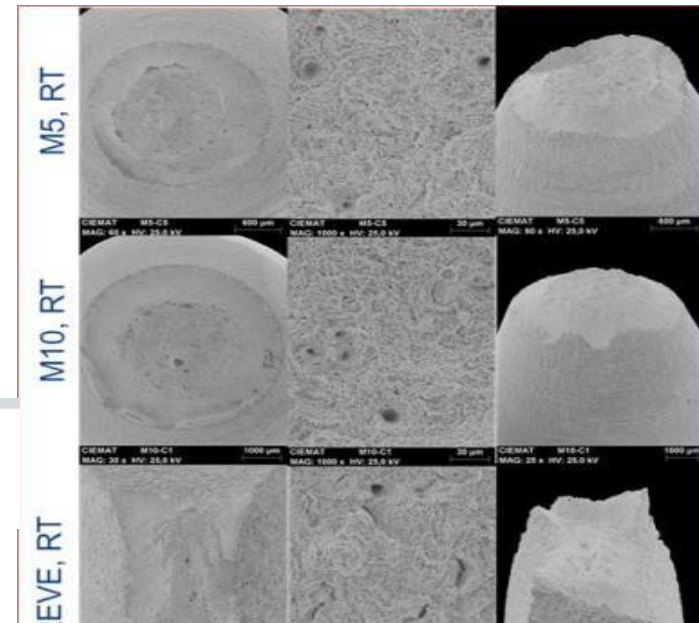
EPRI MRP-417

- In general tensile properties of studied material do not show a significant scatter; even when different specimen geometry is tested

CIE-1 BM A508 C3



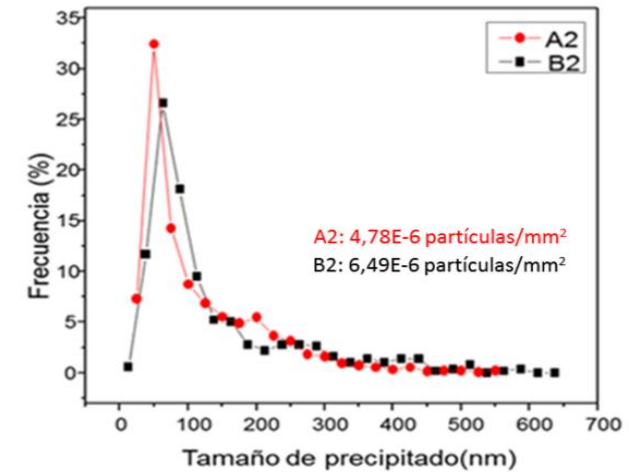
**Ciemat**  
 Centro de Investigaciones  
 Energéticas, Medioambientales  
 y Tecnológicas



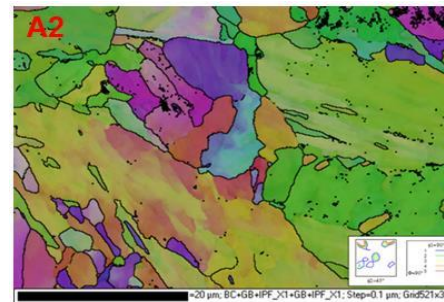
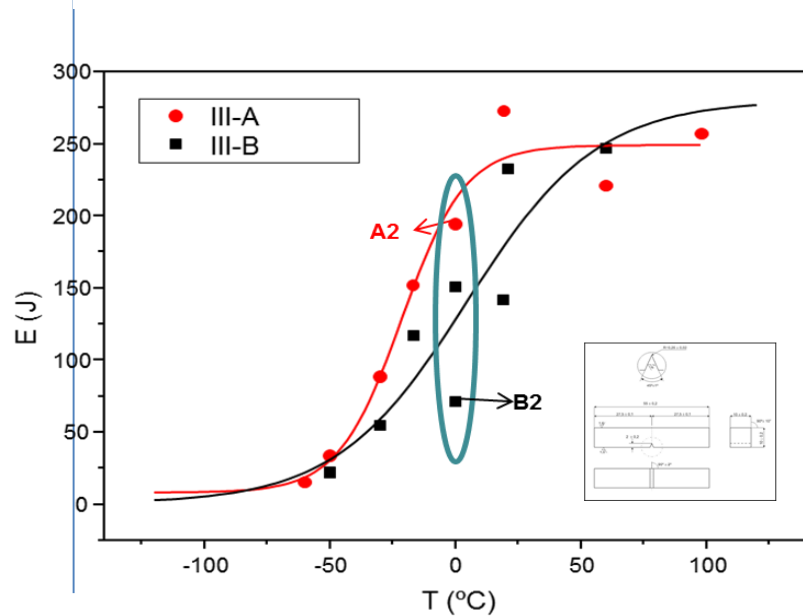
- Impact tests show a dependence of the absorbed energy with the location of the specimens in CIE-1 material

**Ciemat**

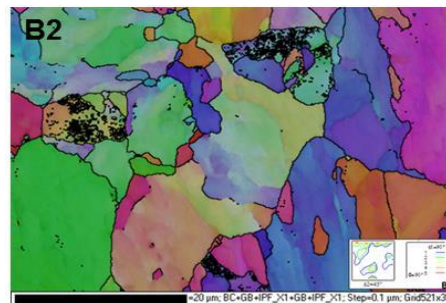
Centro de Investigaciones Energéticas, Medioambientales y Tecnológicas



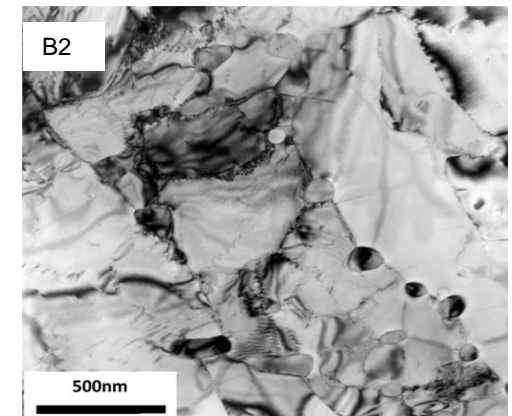
CIE-1 BM A508 C3



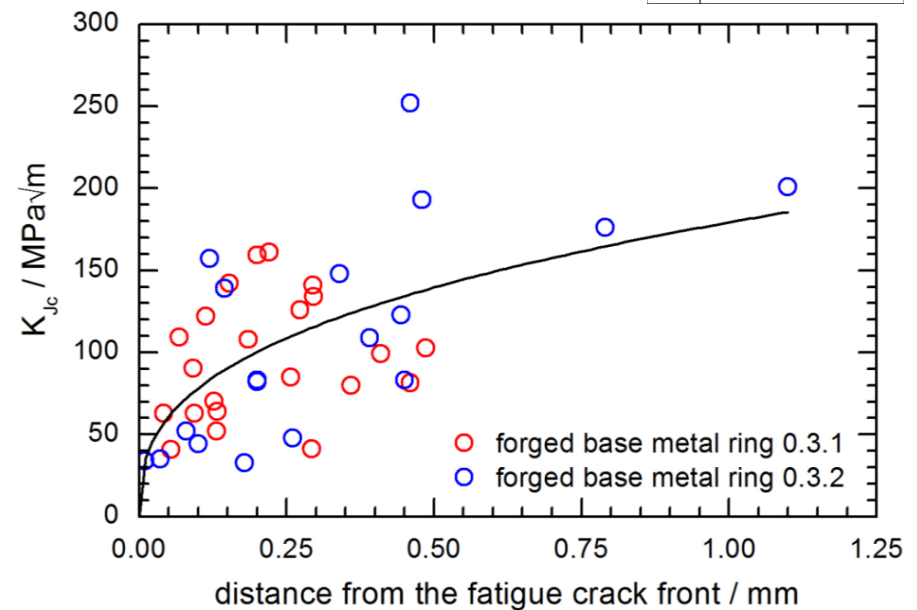
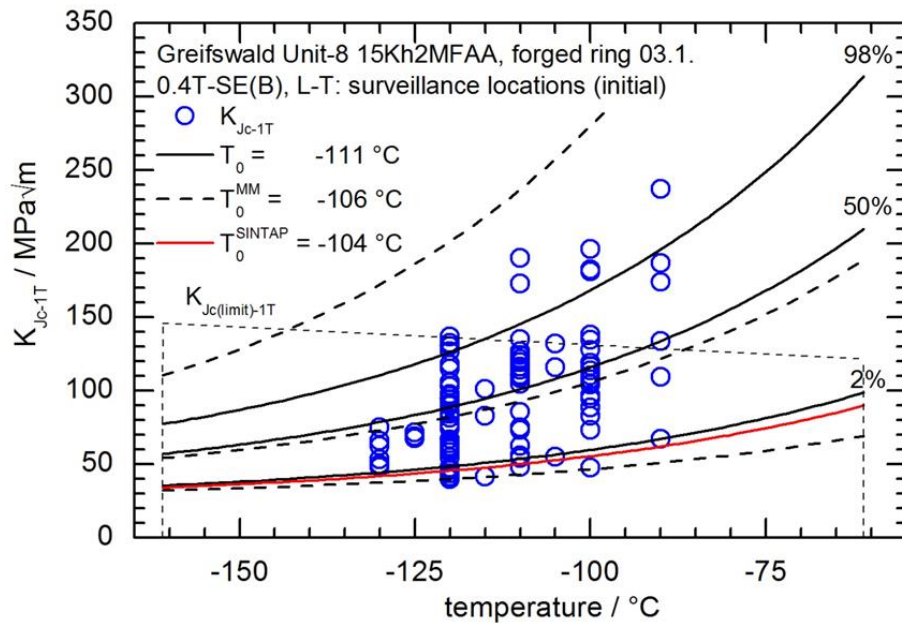
High impact energy



Low impact energy



- Fracture toughness tests show larger scatter than expected for FZD-4 material that could be attributed to the presence of intergranular fracture areas.



# SOTERIA RESULTS

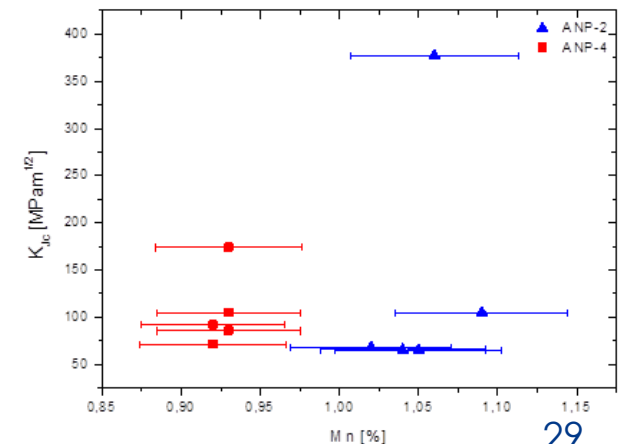
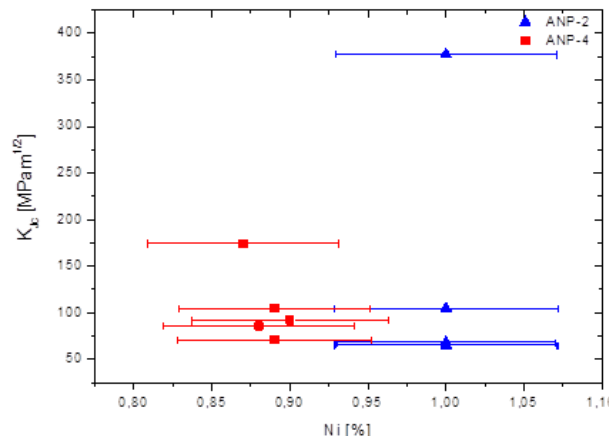
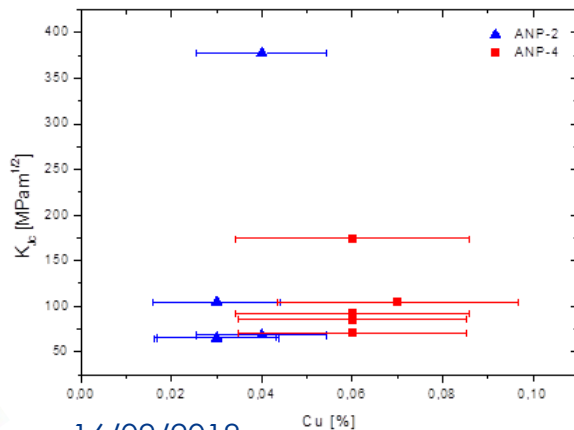
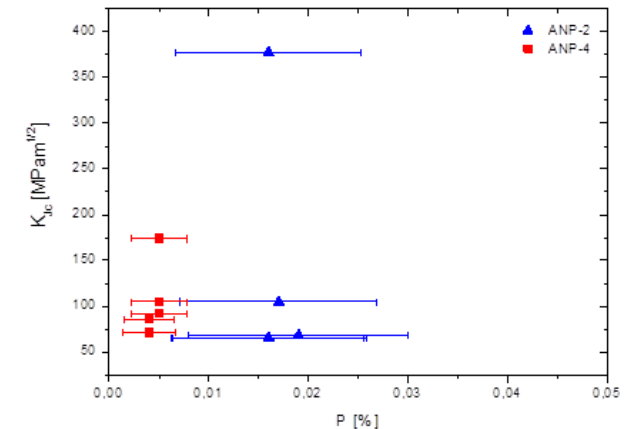


- Based on the chemical analyses performed on unirradiated ANP-2 and ANP-4 materials, using OES method a non-negligible uncertainty in weight % was found for some chemical elements, such as C, P, S, Cu and Ni (in high Ni weld) playing an important role in aging mechanisms of RPV steels.
- Fracture toughness show a dependence on the chemical composition, mainly Mn, Mo, Cr, C and P content

Material	Specimen designation	$K_{IC(1T)}$ in MPa $\sqrt{m}$	T in °C	Cu	Ni	P	Mn	Mo	Cr	C
				in %						
ANP-2	CACS2	65,1	-20	46	7,2	61	5	9,9	8,2	14
	CACS3	68,3	-30	36	7	58	5	10	8,5	13
	CACS4	65,4	-20	44	7,1	60	5	9,8	8,5	14
	CACS5	377,4	-10	36	7,1	58	5	10	8,5	13
	CACS6	104,8	-25	47	7,2	58	5	9,9	8,5	14
ANP-4	TL21	92	-100	43	7	56	4,9	10	8,9	14
	TL22	174,1	-110	43	7	56	5	9,9	9	13
	TL24	85,6	-100	42	7	62	4,9	9,9	9,1	14
	TL28	104,9	-115	38	6,9	56	4,9	9,9	8,9	13
	TL30	71,2	-120	42	7					

ANP-2: Weld metal S3NiMo1/OP41TT  
ANP-4: Base metal 22NiMoCr3-7

framatome



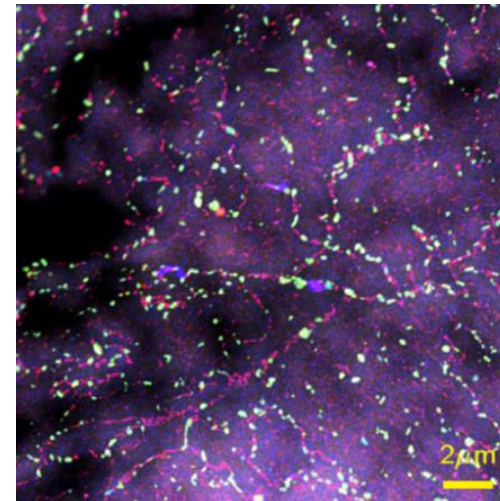
- Microstructural examination of FZD-4 (NPP Greifswald, Unit 8) samples: SEM/EBSD, STEM-HAADF, STEM-EDX



Figures and text replaced by Table

FZD-4 BM 15Kh2MFAA

Type of precipitates	Mean size (nm)	Number density (cm <sup>3</sup> )
V-rich	140	0.38E+14
V-rich (small)	39	0.96E+14
V-rich (very small)	17	2.74E+14
Cr-rich	200	0.10E+14
Carbides	230	0.07E+14
Mo-rich	~500	4.53E+05



STEM-EDX elemental mapping of FZD-4

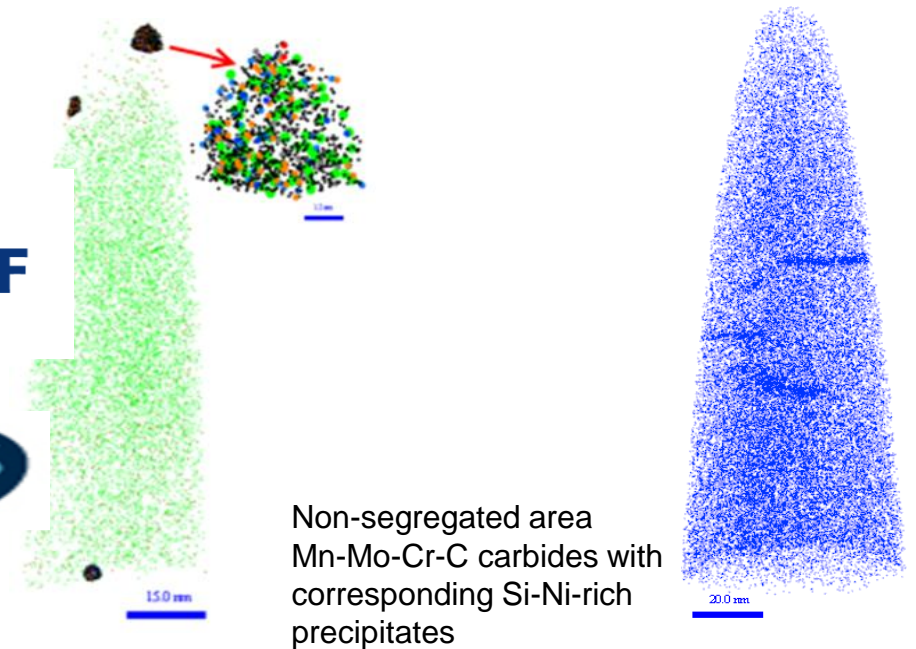
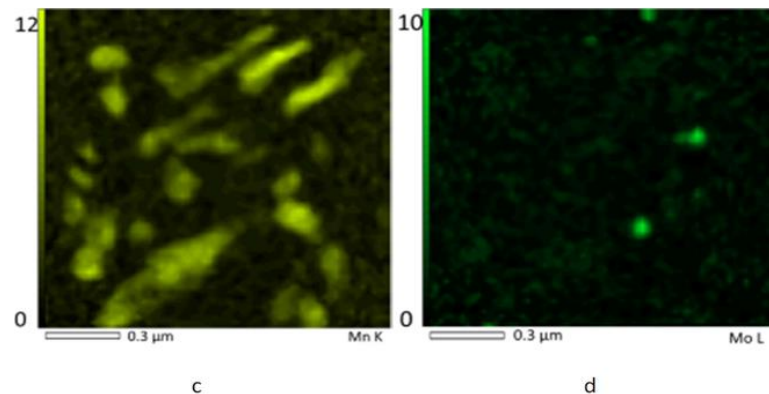
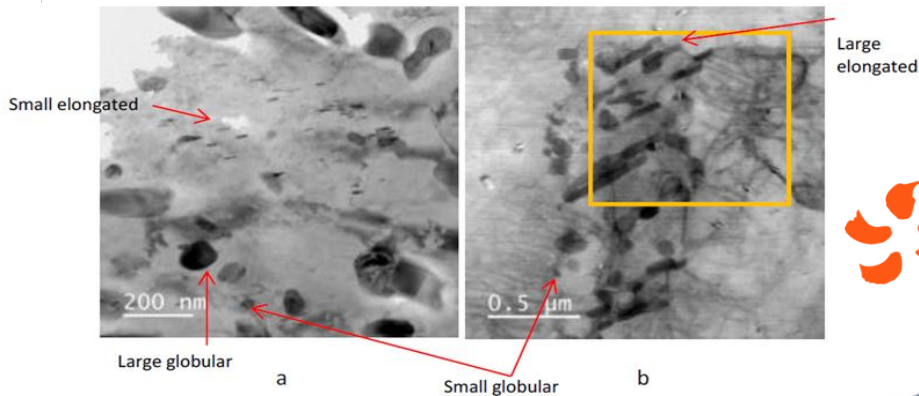
red: V (K $\alpha$ )  
green: Cr (K $\alpha$ )  
blue: Mo (L $\alpha$ )

There are indications of inhomogeneity at different length scales. Phosphorous tends to segregate at grain boundaries. Some kinds of precipitates are also preferentially located at grain boundaries.

## EDF-4 material show micro- and mesoscopic segregations

The distribution of precipitates (carbides) is not homogenous

Formation of Mo, Mn, C - rich clusters was clearly observed on the dislocations in the non-segregated material.



EDF4 samples do not contain characteristic ghost lines, but only micro- and mesoscopic segregations

- ❑ Steel are inhomogeneous materials
- ❑ Scatter in radiation embrittlement can be due to the scatter on the initial condition
- ❑ Main source of scatter in large forgings are related to segregation
- ❑ Scatter on welds can misunderstood radiation effects
- ❑ Inhomogeneity is seen at several scales